Supporting Information: "Twisting and Bending Photo-Excited Phenylethynylbenzenes – A Theoretical Analysis"

Manuel Hodecker,[†] Alexis M. Driscoll,[†,‡] Uwe H. F. Bunz,[¶] and Andreas Dreuw[*,†]

†*Interdisciplinary Center for Scientific Computing, Heidelberg University, Im Neuenheimer Feld 205, D–69120 Heidelberg, Germany*

‡*Department of Chemistry and Biochemistry, University of Notre Dame, Notre Dame, Indiana 46556, USA*

¶*Institute of Organic Chemistry, Heidelberg University, Im Neuenheimer Feld 270, D–69120 Heidelberg, Germany*

E-mail: dreuw@uni-heidelberg.de

Abstract

This supporting information contains geometrical parameters, attachment and detachment density and molecular orbital plots, torsional and bending scans, vibrationally-resolved electronic spectra and spin-orbit coupling constants of the investigated molecules.

1 Geometrical Parameters

The BPEB-HH molecule is shown with numbered C atoms in Figure S1.

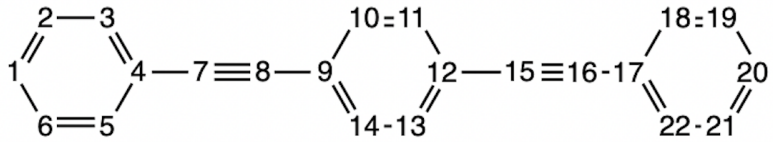

Figure S1: 1,4-Bis(phenylethynyl)benzene (BPEB-HH) with numbered C atoms.

Table S1 demonstrates the effects of changing the orientation of the outer and inner phenyl rings on the central internal coordinates, that is the C7–C8 triple bond, the C8–C9–C10 angle, and the C3–C4–C7 angle. These coordinates correspond to the length of the triple bond, the angle between the triple bond and the inner ring, as well as the angle with the triple bond and the outer ring. They are notable as they are of high subject to modification in optimization and torsion. In rotation of the outer ring, the coordinates of the triple bond closest to the twisted phenyl ring were investigated. It can be seen that the twisting of both the middle and outer rings have little to no effect on the geometry of the molecule, and that these bond lengths and angles are very close to standard values. In comparison to tolan, BPEB-HH is similar as twisting the rings has little to no effect on the triple bond length, but is different as the planar equilibrium triple bond length is 0.04 Å less than that of tolan in the electronic ground state.[1]

Table S1: Central internal coordinates of BPEB-HH at different torsion angles in the electronic ground state.

Coordinate	Planar	Mid Twist	Side Twist
C7–C8 Bond [Å]	1.20	1.20	1.20
C8–C9–C10 Angle [°]	120.68	120.63	120.62
C3–C4–C7 Angle [°]	120.51	120.48	120.48

For BPEB-FH and BPEB-FF, the same numbering of the C atoms applies as for BPEB-HH in Figure S1. The C8–C9–C14 angle and the C5–C4–C7 angle were investigated in

addition to the C7–C8 triple bond, the C8–C9–C10 angle, and the C3–C4–C7 angle, as they take into account the change in angle both closer to and further from the fluorine substituent. As can be seen in Table S2, the twisting of both the middle and outer rings have slight effects on the geometry of the BPEB-FH and BPEB-FF molecules, but greater than that of BPEB-HH. For BPEB-FH, the length of the triple bond does not change, but the triple bond and outer phenyl ring shift up to 0.23° away from the fluorine substituent, which happens more so with torsion of the middle ring than the outer ring. There is about a 1° difference in the BPEB-HH and BPEB-FH C8–C9–C10 bond angles for both planar and twisted versions of the molecule. For BPEB-FF, the length of the triple bond does not change, but the triple bond and outer phenyl ring shift up to 0.17° away from the fluorine substituent. There is a nearly 1.5° difference of C8–C9–C10 bond angles of BPEB-HH and BPEB-FF. The placement of the fluorine substituents causes negligible changes in the geometry of the molecule.

Table S2: Central internal coordinates of BPEB-FH and BPEB-FF at different torsion angles in the electronic ground state.

	BPEB-FH			BPEB-FF		
Coordinate	Planar	Mid Twist	Side Twist	Planar	Mid Twist	Side Twist
C7–C8 Bond [Å]	1.20	1.20	1.20	1.20	1.20	1.20
C8–C9–C10 Angle [°]	121.67	121.52	121.52	122.04	121.87	121.90
C8–C9–C14 Angle [°]	121.13	121.19	121.22	120.41	120.50	120.50
C3–C4–C7 Angle [°]	120.60	120.37	120.41	120.60	120.41	120.41
C5–C4–C7 Angle [°]	120.23	120.44	120.40	120.24	120.40	120.41

2 Attachment and Detachment Densities

In Figure S2, attachment and detachment density[2] plots of the S_1 state of planar, mid- and side-twisted BPEB-HH are shown.

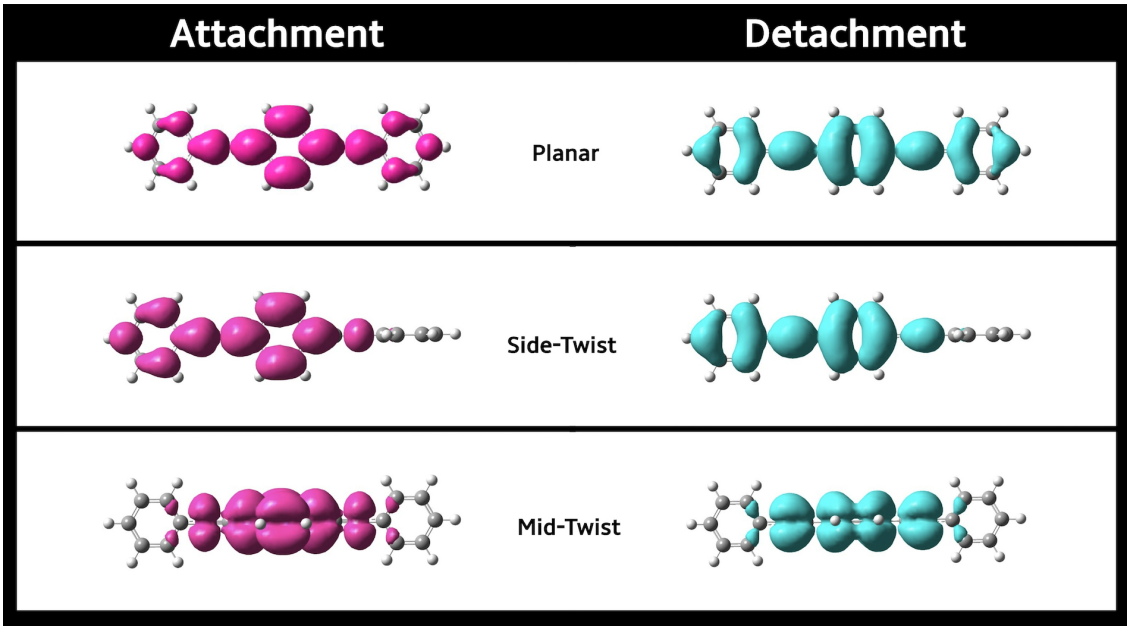

Figure S2: Attachment (left) and detachment (right) densities of the S_1 state of planar, side-twisted, and mid-twisted BPEB-HH calculated at the level of CAM-B3LYP/def2-TZVP.

3 Molecular Orbitals

Molecular orbital (MO) pictures contributing to states with a non-vanishing oscillator strength of BPEB-FH and BPEB-FF are shown in Figures S3 and S4 together with the corresponding amplitude in the excitation vector.

The changes of the MOs when going from the linear to the *trans*-bent geometry in both the planar and orthogonal configuration of BPEB-HH are shown in Figure S5.

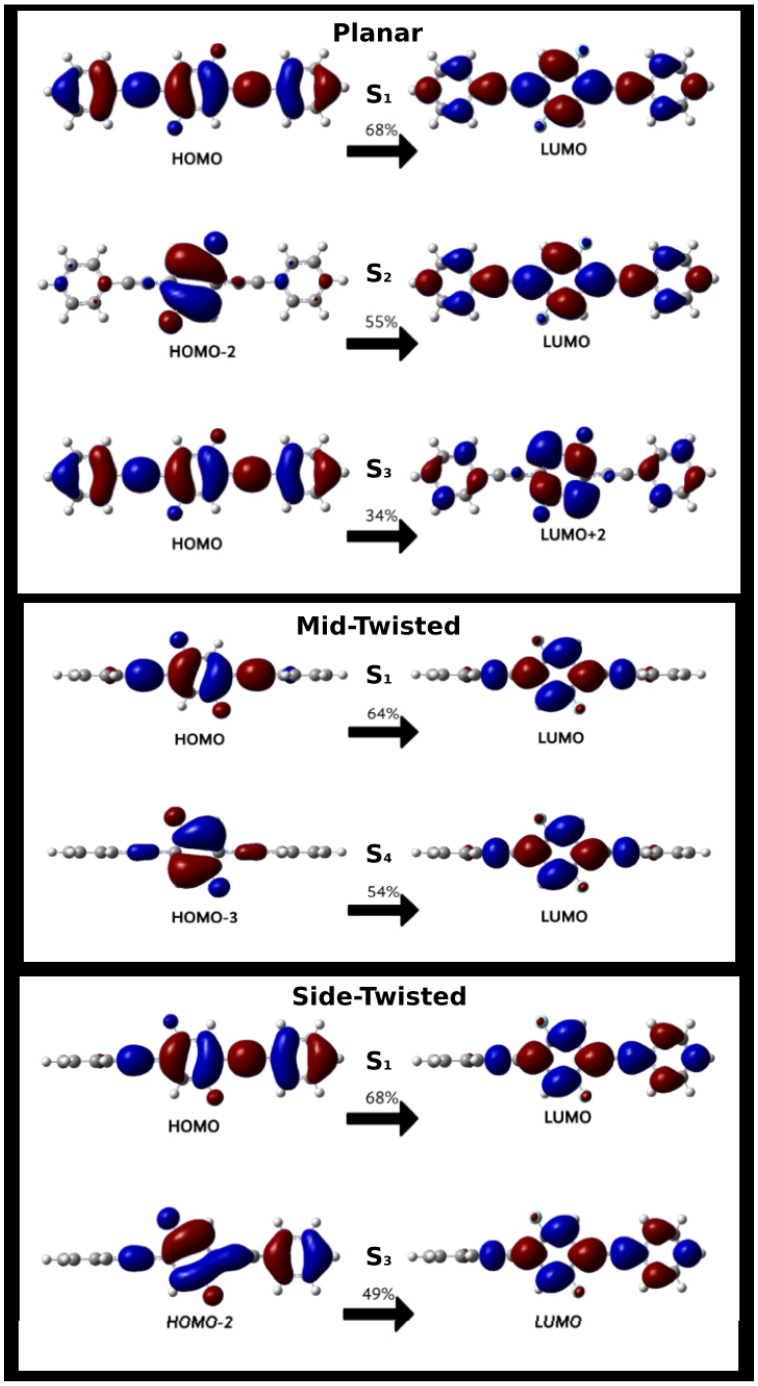

Figure S3: Molecular orbitals contributing to the vertical excited S_1, S_2, and S_4 states of planar BPEB-FH (top), S_1 and S_4 states of orthogonally mid-twisted BPEB-FH (middle), and the S_1 and S_3 states of orthogonally side-twisted BPEB-FH (bottom), all of which have non-vanishing oscillator strength.

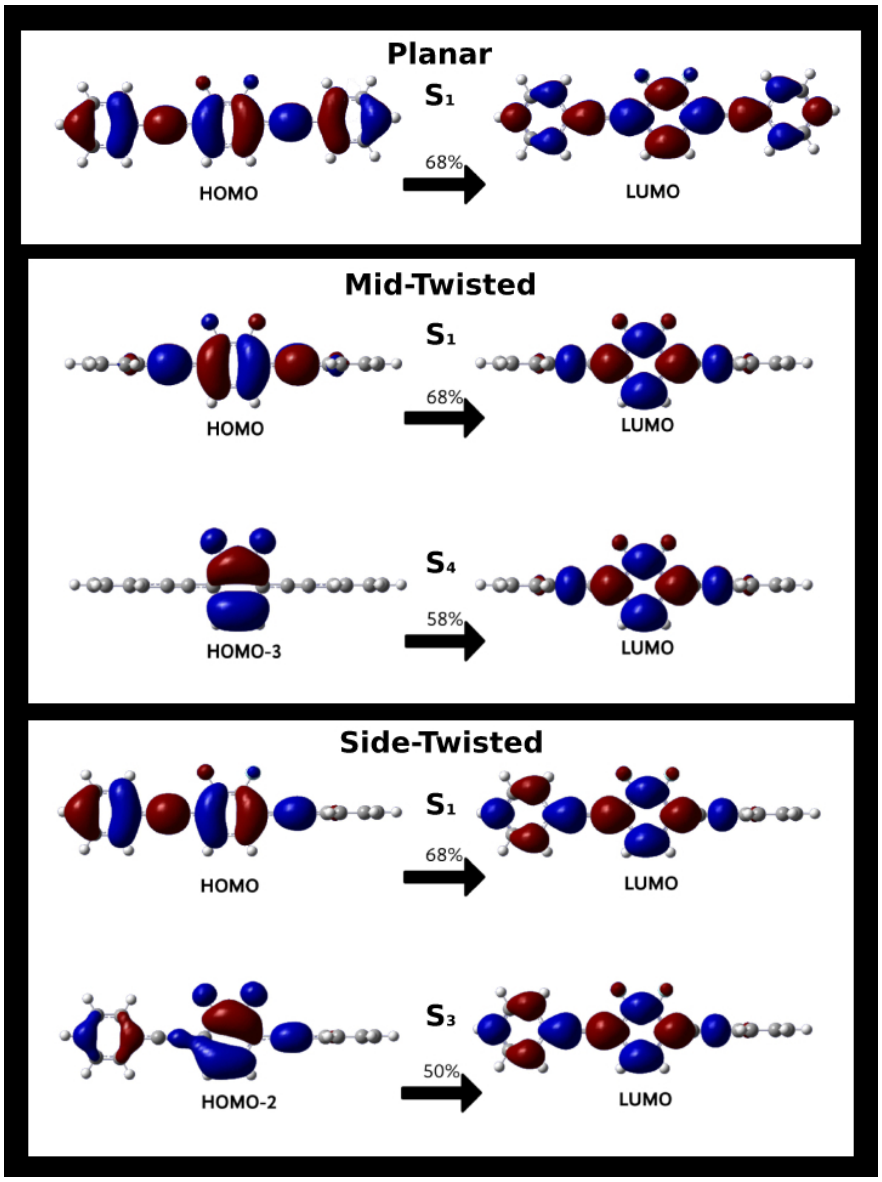

Figure S4: Molecular orbitals contributing to the vertical excited S_1 state of planar BPEB-FF (top), S_1 and S_4 states of orthogonally mid-twisted BPEB-FF (middle), and the S_1 and S_3 states of orthogonally side-twisted BPEB-FF (bottom), all of which have non-vanishing oscillator strength.

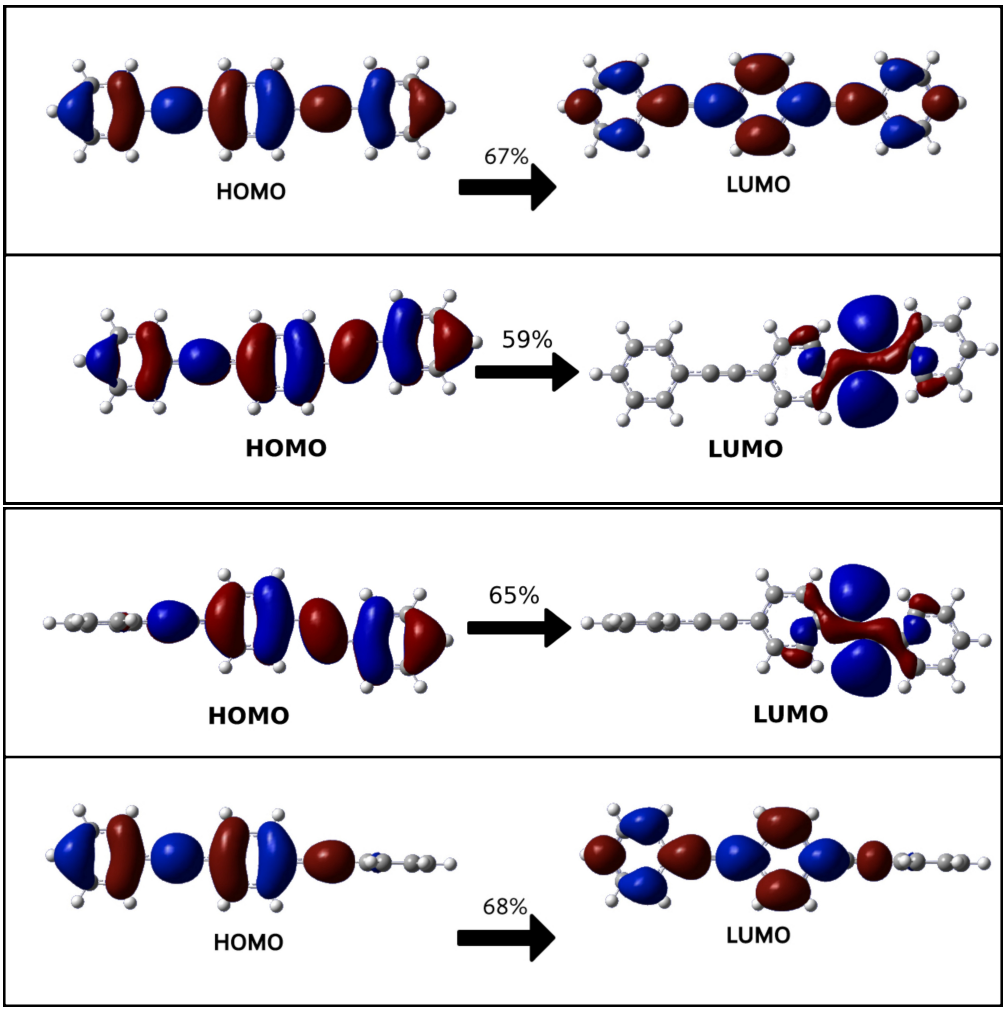

Figure S5: Comparison of the molecular orbitals involved in the $S_0 \rightarrow S_1$ transition when going from the linear to the *trans*-bent structure of BPEB-HH in both the planar (top) and orthogonal (bottom) configuration.

4 Torsional Scans of BPEB-FH and BPEB-FF

Relaxed scans of the excited states of BPEB-FH and BPEB-FF along the torsional mode of the side- and mid-ring are shown in Figures S6 and S7. For the outer twist, the torsional scan was carried out with the dihedral angle to the inner phenyl ring kept frozen, whereas for the inner twist, the two dihedral angles to the outer phenyl rings were kept frozen.

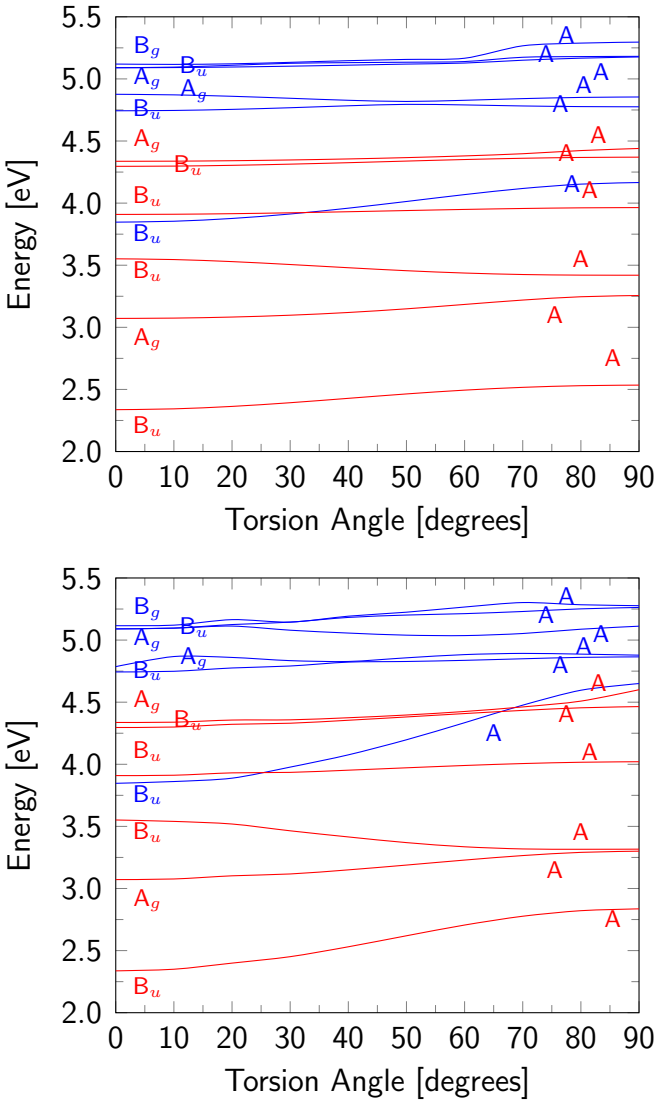

Figure S6: Potential energy surfaces of excited singlet (blue) and triplet (red) states along the relaxed scan of side-twisted (top) and mid-twisted (bottom) BPEB-FH in the S_0 state at the CAM-B3LYP/def2-TZVP level of theory. The states are labeled according to the C_{2h} point group on the left.

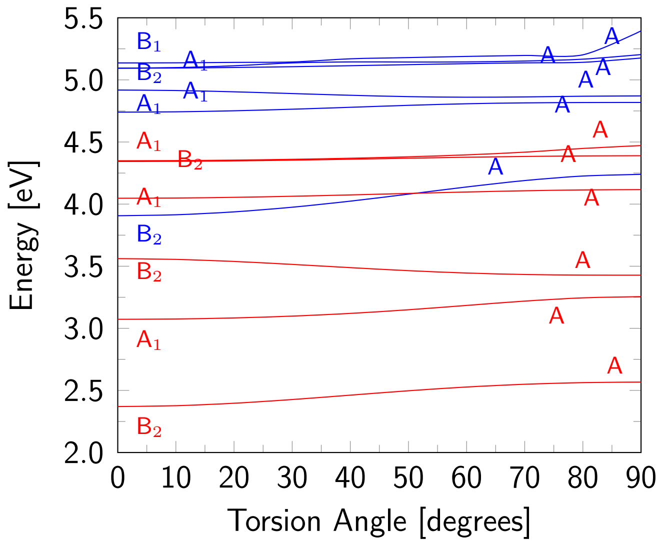

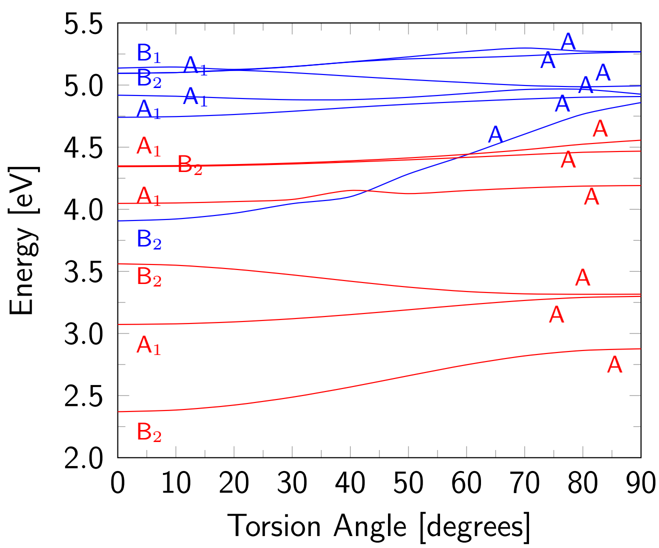

Figure S7: Potential energy surfaces of excited singlet (blue) and triplet (red) states along the relaxed scan of side-twisted (top) and mid-twisted (bottom) BPEB-FF in the S_0 state at the CAM-B3LYP/def2-TZVP level of theory. The states are labeled according to the C_{2v} point group on the left.

5 Rigid Torsional Scans

Potential energy surfaces of excited singlet and triplet states along a rigid torsional scan in the electronic ground state of BPEB-HH, BPEB-FH and BPEB-FF are shown in Figures S8, S9 and S10, respectively. The results are seen to be extremely similar to the relaxed scans, thus allowing for rigid scans as a good approximation to relaxed ones.

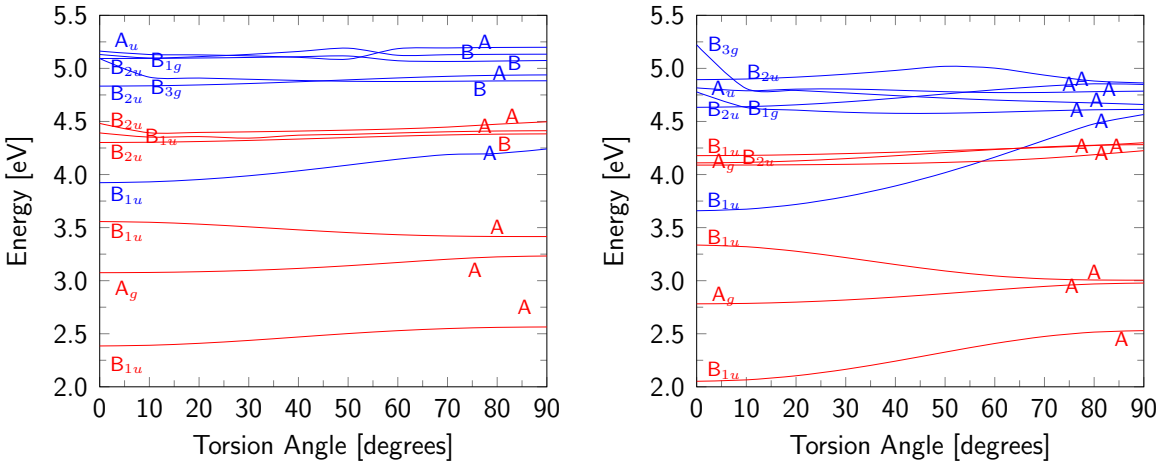

Figure S8: Potential energy surfaces of excited singlet (blue) and triplet (red) states along the rigid scan of side-twisted (left) and mid-twisted (right) BPEB-HH in the electronic ground state at the CAM-B3LYP/def2-TZVP level. The energy is given relative to the ground state in its equilibrium geometry, respectively. The states are labeled according to the D_{2h} point group on the left, and according to the C_2 point group on the right.

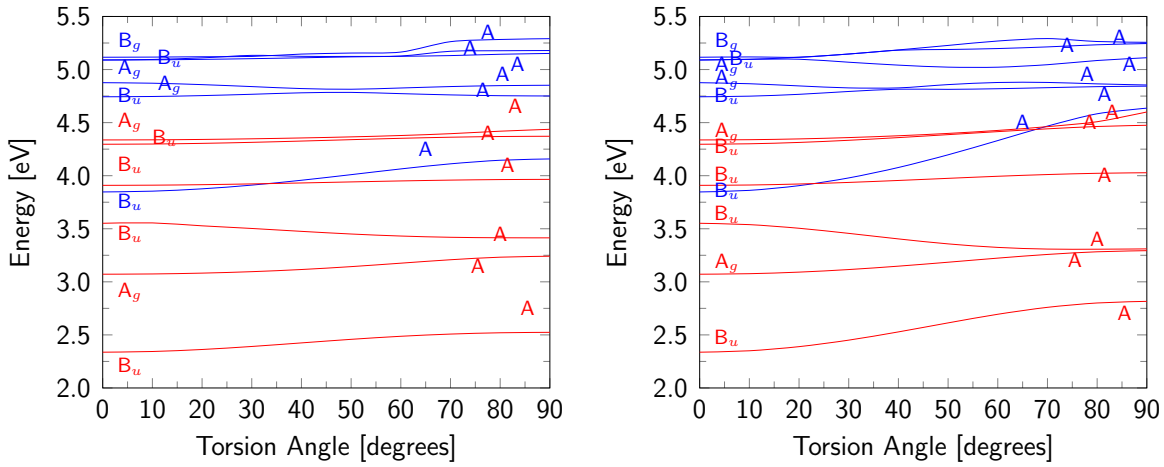

Figure S9: Potential energy surfaces of excited singlet (blue) and triplet (red) states along the rigid scan of side-twisted (left) and mid-twisted (right) BPEB-FH in the electronic ground state at the CAM-B3LYP/def2-TZVP level. The energy is given relative to the ground state in its equilibrium geometry, respectively. The states are labeled according to the C_{2h} point group on the left.

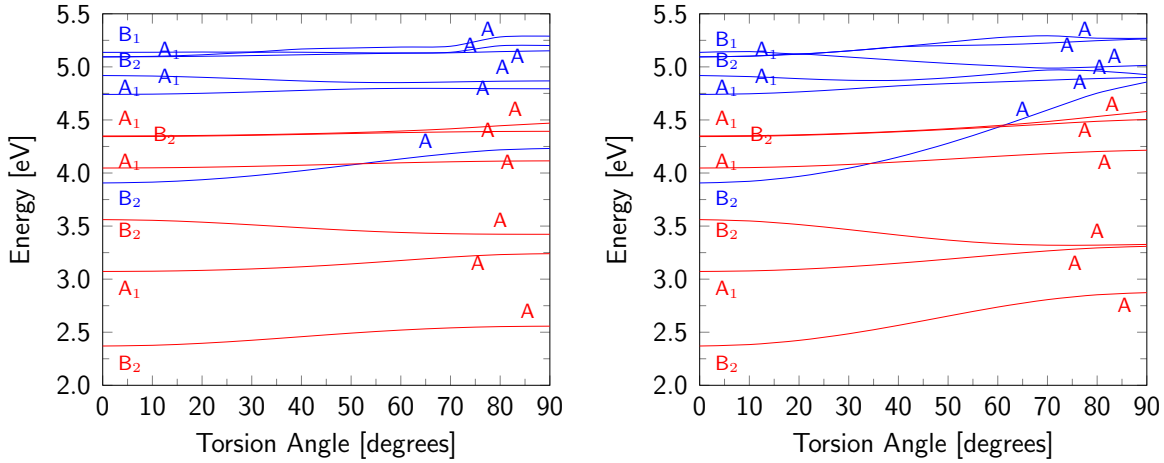

Figure S10: Potential energy surfaces of excited singlet (blue) and triplet (red) states along the rigid scan of side-twisted (left) and mid-twisted (right) BPEB-FF in the electronic ground state at the CAM-B3LYP/def2-TZVP level. The energy is given relative to the ground state in its equilibrium geometry, respectively. The states are labeled according to the C_{2v} point group on the left.

6 Vibrationally-Resolved Electronic Spectra

Vibrationally-resolved absorption and emission spectra[3] of BPEB-FH and BPEB-FF are shown in Figures S11–S13. Note that no experimental absorption spectrum of BPEB-FF

was available. These theoretical spectra were also computed in chloroform, using the C-PCM solvation model,[4] but were found not to improve compared to experiment.

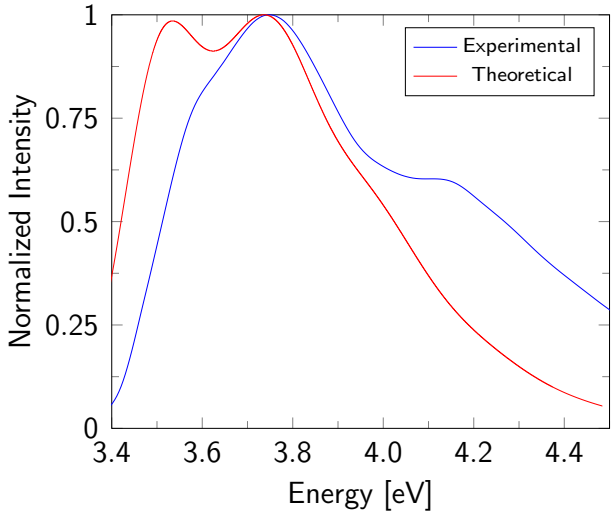

Figure S11: Comparison of the experimental and simulated absorption spectra of the first excited S_1 state of planar BPEB-FH. The theoretical spectrum is an Adiabatic Hessian Franck-Condon spectrum with a half-width of 0.09 eV calculated at the level of TDDFT/CAM-B3LYP/def2-TZVP.

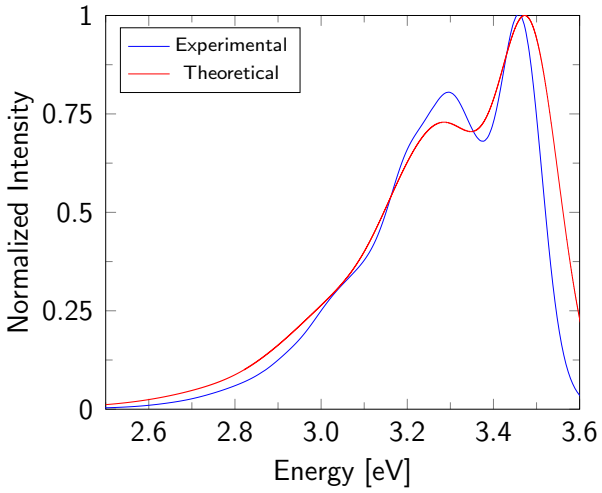

Figure S12: Comparison of the experimental and simulated emission spectra of the first excited S_1 state of planar BPEB-FH. The theoretical spectrum is an Adiabatic Hessian Franck-Condon spectrum with a half-width of 0.08 eV calculated at the level of TDDFT/CAM-B3LYP/def2-TZVP.

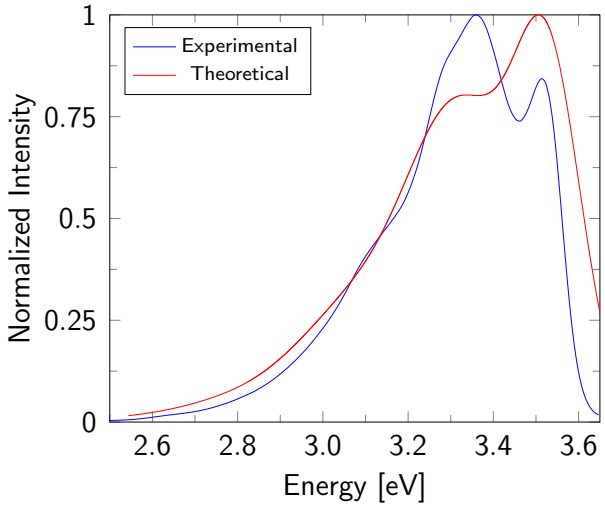

Figure S13: Comparison of the experimental and simulated emission spectra of the first excited S_1 state of planar BPEB-FF. The theoretical spectrum is an Adiabatic Hessian Franck-Condon spectrum with a half-width of 0.09 eV calculated at the level of TDDFT/CAM-B3LYP/def2-TZVP.

7 Spin-Orbit Coupling Constants

Spin-orbit coupling (SOC) constants[5] for twisted BPEB-FH and BPEB-FF calculated using the one-electron Breit–Pauli Hamiltonian at the TDDFT/CAM-B3LYP/def2-TZVP level of theory as implemented in Q-Chem 5.2 are shown in Tables S3 and S4.

Table S3: Computed SOC constants between the BPEB-FH excited S_1 state and the triplet states that are crossed along the nearest optimized twisting angle at the crossing point.

Ring Twisted	Crossing	Angle [°]	SOC [cm^{-1}]
side	S_1/T_4	30	0.51
middle	S_1/T_4	30	0.65
middle	S_1/T_5	70	0.65
middle	S_1/T_6	70	0.03

Table S4: Computed SOC constants between the BPEB-FF excited S_1 state and the triplet states that are crossed along the nearest optimized twisting angle at the crossing point.

Ring Twisted	Crossing	Angle [°]	SOC [cm^{-1}]
side	S_1/T_4	50	0.51
middle	S_1/T_4	40	0.44
middle	S_1/T_5	60	0.01
middle	S_1/T_6	60	0.15

8 Bending Scans

The ground-state energy profile of bending BPEB-HH with the third phenyl ring either planar or orthogonal to the other two are shown in Figure S14.

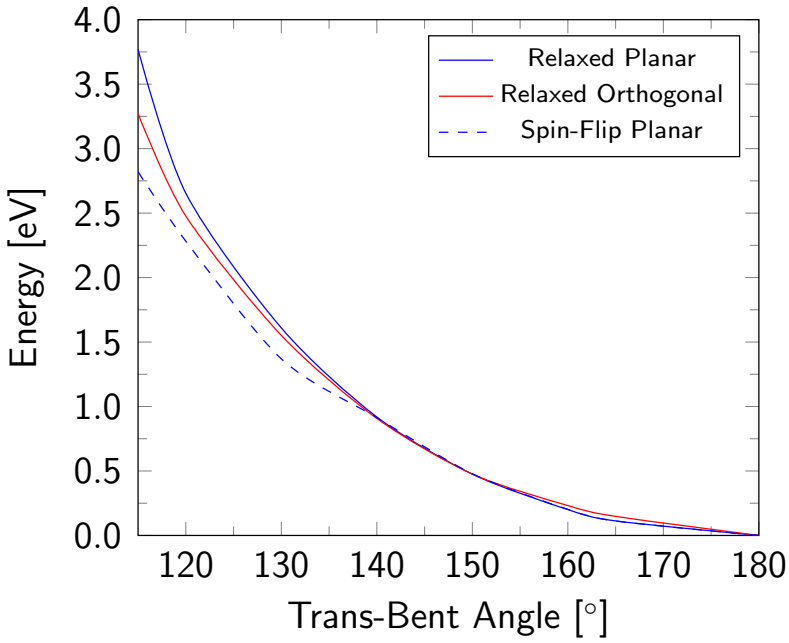

Figure S14: Ground-state energy profile of bending of BPEB-HH, with either a planar or orthogonal outer ring, calculated either from a relaxed scan at the closed-shell CAM-B3LYP/def2-TZVP level of theory or at the open-shell SF-TDDFT/TDA/CAM-B3LYP/def2-TZVP level of theory with geometries from the closed-shell relaxed scan used.

In addition to the restricted closed-shell calculation, an unrestricted spin-flip (SF) TDDFT calculation[6] within the Tamm–Dancoff approximation[7] (TDA) has been performed for the planar system with geometries taken from the costraint closed-shell optimizations. The ground state energies can be seen in Figure S14, where it is denoted as "Spin-Flip Planar". The results of the SF-TDDFT/TDA and standard TDDFT calculations at the CAM-B3LYP/def2-TZVP level of theory are found to be nearly identical up to an angle of about 140°, then they start to differ slightly. At the SF-TDDFT level, the expectation value of the total spin operator $\hat{S}^2$ in the linear structure is $\langle \hat{S}^2 \rangle = 0.109$ in the "true" ground state, exemplifying slight spin contamination. The $\langle \hat{S}^2 \rangle$ values for other angles of bending are 0.110 for 165° and 160°, 0.112 for 150°, 0.117 for 140°, 0.058 for 130°, and 0.060 for 120°

and 115°. There is slight spin-contamination for all angles of bending, but the $\langle \hat{S}^2 \rangle$ value is an average of 0.05 smaller for bending angles of 130°, 120°, and 115° compared to the linear structure. This is peculiar as there is greater deviation of the open-shell ground state from the closed-shell ground state at these angles.

References

(1) Krämer, M.; Bunz, U. H. F.; Dreuw, A. Comprehensive Look at the Photochemistry of Tolane. *J. Phys. Chem. A* **2017**, *121*, 946–953.

(2) Head-Gordon, M.; Grana, A. M.; Maurice, D.; White, C. A. Analysis of Electronic Transitions as the Difference of Electron Attachment and Detachment Densities. *J. Phys. Chem.* **1995**, *99*, 14261–14270.

(3) Biczysko, M.; Bloino, J.; Santoro, F.; Barone, V. In *Computational Strategies for Spectroscopy: From Small Molecules to Nano Systems*; Barone, V., Ed.; John Wiley & Sons, Ltd, 2012; Chapter 8, pp 361–443.

(4) Cossi, M.; Rega, N.; Scalmani, G.; Barone, V. Energies, structures, and electronic properties of molecules in solution with the C-PCM solvation model. *J. Comput. Chem.* **2003**, *24*, 669–681.

(5) Marian, C. M. Spin-Orbit Coupling in Molecules. *Rev. Comput. Chem.* **2001**, *17*, 99–204.

(6) Shao, Y.; Head-Gordon, M.; Krylov, A. I. The spin–flip approach within time-dependent density functional theory: Theory and applications to diradicals. *J. Chem. Phys.* **2003**, *118*, 4807–4818.

(7) Hirata, S.; Head-Gordon, M. Time-dependent density functional theory within the Tamm–Dancoff approximation. *Chem. Phys. Lett.* **1999**, *314*, 291–299.